Acoustic Emission Measurements during Unconfined Compression of Diorite Samples

Carola WIESER *, Lisa WILFING *, Heiko KÄSLING *, Manuel RAITH **,
Ronald RICHTER **, Franziska GEMANDER **, Dorothee MOSER **,
Christian U. GROSSE **, Kurosch THURO *
* Technische Universität München, Chair for Engineering Geology, Munich, Germany
** Technische Universität München, Chair of Non-destructive Testing, Munich, Germany

Abstract. The influence of stress-induced microcracking on rock strength is one of the key questions in rock mechanics, especially for applications in mining and tunneling. Here, we present first results from unconfined compression testing combined with acoustic emission monitoring on two diorite samples. The objective was to gain information about the influence of experimental setup on acoustic emissions during unconfined compression. With the analysis of acoustic events, it is possible to determine the initiation and propagation of microcracks with regard to loading conditions and deformation rates. In our study, the combined analysis of stress-strain curve and event rate allowed a determination of main deformation stages during loading. Results from 3D source localization indicated a conjugate shear system which is typical for unconfined compression tests although the failure pattern did not show the expected hourglass form. An elevated number of events occurred at the end surfaces of the rock. They resulted from friction at the loading plates and can be eliminated by using PTFE plates between rock and loading plates. As the slope of the stress-strain curve was strongly affected by the PTFE plates, thinner PTFE foils will be applied in future tests.

1. Introduction

Microseismic events in underground openings may cause severe stability problems in mines or tunnels and are therefore monitored carefully especially in mining. They occur as a result of fractures forming due to a redistribution of primary stresses around the opening and a relaxation of the rock mass after excavation [1] [2].

At rock scale, the same processes take place during excavation. Stress-induced microcracks and macrofractures develop and damage the rock around the excavation boundary. Changes in rock mechanical properties have great influence on penetration rates in TBM tunnelling. Our objective is to improve the model for a prediction of penetration rates in mechanised tunnelling. For a reliable penetration prediction model a better understanding of the deformation behaviour of rocks is necessary.

One of the main input parameters in penetration prediction models is the uniaxial compressive strength of rocks which is strongly affected by the evolution of microcracks. In this study, uniaxial compressive strength as well as the deformation behaviour of rock are analysed using acoustic emissions (AE) for the determination of microcracking during loading of rock samples.

We present results from AE measurements on brittle rocks during unconfined compression. A signal-based analysis as well as a 3-dimensional localization of AE events was performed and main deformation stages in the stress-strain curve could be estimated from AE according to the methods of Bieniawski [3] and Martin [4].

2. Experimental Setup

2.1 Unconfined Compression Testing

We tested two specimens of homogeneous, porphyritic, fine- to medium-grained diorite from Nittenau, south-east Germany (Bavarian Forest), containing mainly feldspars, biotite and quartz (Fig. 1). Samples were prepared for testing with a diameter of 8 cm and a height H to diameter D ratio of H/D = 2 [5]. Uniaxial loading was applied under servo-control at a constant velocity rate of 0.1 mm/min. During the tests, axial strain was measured by position sensors installed between the loading plates. Sample NIT-1 was loaded three times using polytetrafluoroethylene (PTFE, aka Teflon®) plates in order to reduce friction at the loading plates. During the last cycle, when the sample was loaded until failure, no attenuating materials were applied and no AE were monitored in order not to destroy the transducers. In a second test, sample NIT-2 was loaded until failure according to Mutschler [5] without using PTFE plates but with recording of AE.

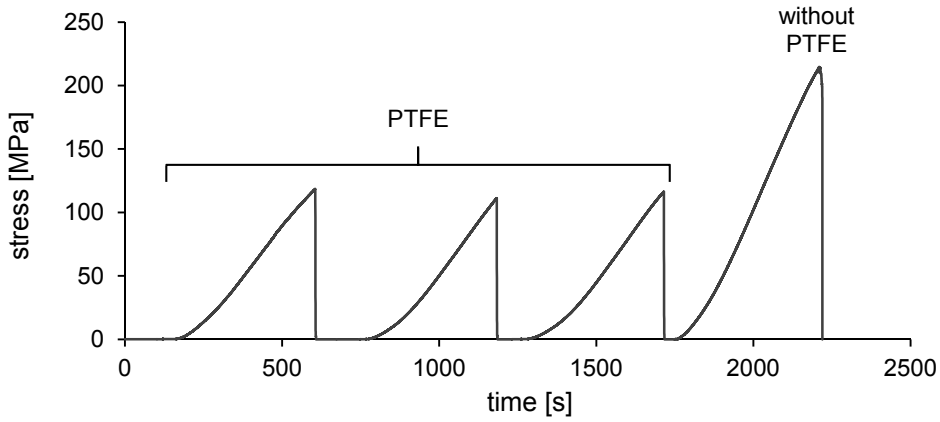

Fig. 1. Repeated loading of sample NIT-1, first 3 cycles applying 2.8 cm thick PTFE plates between loading plates and the last cycle until failure without PTFE.

2.2 Acoustic Emission Testing

For AE monitoring during unconfined compression testing, 14 piezoelectric transducers were attached to the sample surface recording elastic waves originating from the formation of microcracks inside the rock. Another two guard sensors were attached to the loading plates and recorded background noises coming from the hydraulic device (experimental setup shown in Fig. 2). The pre-amplification system included a bandpass filter with a frequency range of 10 kHz to 1 MHz. Thus, low frequencies originating from the hydraulic pump of the loading frame were eliminated. We used a pre-amplification between 27 and 33 dB for three different types of sensors in order to receive similar signals. AE were recorded by an automatic data acquisition system (TranAX by Elsys) using a sampling frequency of 5 MHz. In order to avoid huge amounts of data, signals were not recorded continuously. Instead we applied a slew rate trigger and a ring buffer storing only the events exceeding the trigger conditions.

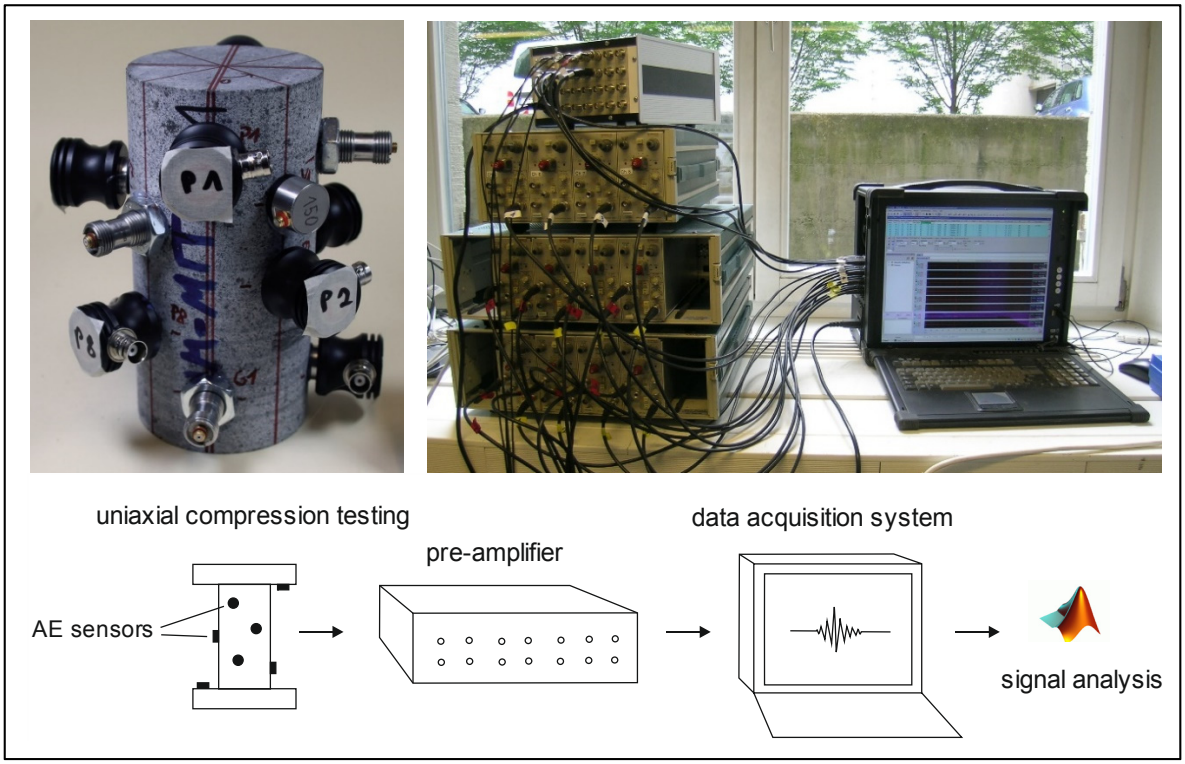

Fig. 2. Experimental setup of AE instrumentation and data acquisition system.

3. Data Analysis

Data analysis was carried out using the software SquirrelAE which was developed at the Chair of Non-destructive Testing at Technische Universität München. Using a signal-based AE method, recorded waveforms were analysed. The software includes an algorithm for automatic p-wave arrival detection based on the Akaike Information Criterion (AIC). The accuracy of the onset detection process is critical for a reliable localization of AE events [6]. After picking arrival times, signal parameters like hitrate, signal to noise ratio, signal energy, rising time, maximum amplitude as well as the frequency can be analysed.

For a 3D-localization of events, the Bancroft algorithm was used which was developed to solve global positioning system (GPS) equations [7]. In addition, the iterative algorithm of Geiger [8] was applied which was originally established for the localization of earthquakes. Kurz [9] gives an overview of several localization algorithms and their scope of application for localizing acoustic events. According to Kurz, the algorithm providing the best results is dependent on boundary conditions and sensor covering. For our tests the Bancroft algorithm usually delivered the best results.

4. Experimental Results

4.1 Test 1: Friction at loading plates

In a first test, the influence of PTFE as a means for minimizing friction between end surfaces and loading plates was tested during unconfined compression. Two PTFE sheets of 2.8 mm thickness were inserted between rock specimen and loading plates in order to reduce acoustic signals resulting from friction at the end surfaces. The rock sample NIT-1 was loaded three times with PTFE and once without the material. The influence of the material was visible as a decrease in the slope of the recorded stress-strain-curve, resulting in a Young's modulus

60% lower when PTFE was applied (Table 1). As a proper determination of rock mechanical parameters was not possible with the attenuating effect of the material, subsequent tests were carried out without PTFE. The effects and the usability of PTFE material for a reduction of end effects is investigated more thoroughly in ongoing tests. First results show that thinner PTFE foils (0.25 mm) have less influence on the stress-strain curve. The effect on AE has to be analysed in more detail.

Table 1. Changes in Young's modulus during repeated loading with and without using PTFE plates.

Young's modulus [GPa] *with* PTFE			**Young's modulus [GPa] *without* PTFE**
1. loading	2. loading	3. loading	4. loading (until failure)
31,4	32,5	32,7	54,1

4.2 Test 2: Microcracking and deformation behaviour

4.2.1 Deformation behaviour

A second uniaxial compression test was performed with constant loading until failure. From the number of AE events, different stages of crack development could be determined according to Bieniawski [3]. The results are shown in Fig. 3 where all detected acoustic events are plotted without filtering. According to Eberhardt et al. [10], the first deformation stage (A) is characterized by the closure of existing cracks aligned at an angle to the load whereas parallel cracks may open. The stress-strain curve is non-linear during this deformation stage. In our test, the crack closure threshold σ_{cc} can be set at about 31 % the peak strength (σ_c), which is 218 MPa.

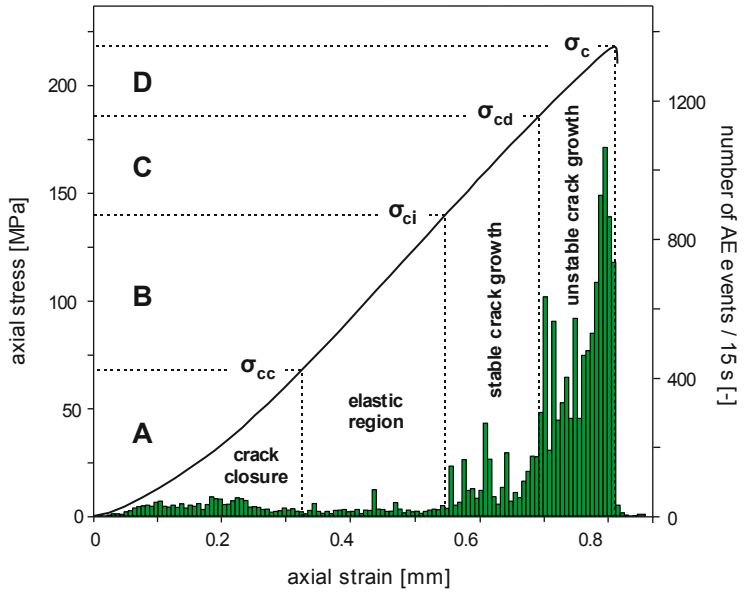

Fig. 3. Stress-strain curve from constant loading with deformation stages (A-D) and crack development determined from the characteristics of the curve and the number of AE events.

The second stage (B) is marked by the linear section of the stress-strain curve where elastic deformation occurs. Only a few acoustic emissions were recorded during this stage. Event numbers increase again at a stress level of about 0.64 σ_c which represents the crack initiation threshold σ_{ci} where stable crack growth takes place [3]. According to Cai et al. [11], the crack initiation threshold of most rocks usually is in the range between 0.3 to 0.5 σ_c which is clearly lower than what our test revealed. A significant increase in events and an overall

high AE activity indicates the onset of unstable crack growth and crack coalescence (D). This phase begins at a crack damage threshold σ_{cd} of about 0.85 σ_c in our test and thus is more consistent with existing studies which state a σ_{cd} between 0.7 and 1.0 σ_c [11]. With a combined analysis of the volumetric strain curve, a more precise determination of stress levels can be achieved. Thus, circumferential strain measurements will be implemented in future experiments. Immediately after the first failure occurred, the test was stopped in order not to destroy the AE sensors. Events continued for about 30 seconds after the applied load was removed as the relaxation of rock may also result in microcracking and AE.

4.2.2 Localization of events

In the following, results from localization are presented. Fig. 4 shows 3D plots of localized AE summarising events in the different stages of deformation (A-D, see Fig. 3). From all signals only those events localized using the Bancroft algorithm and with a correlation coefficient higher than 0.5 were plotted.

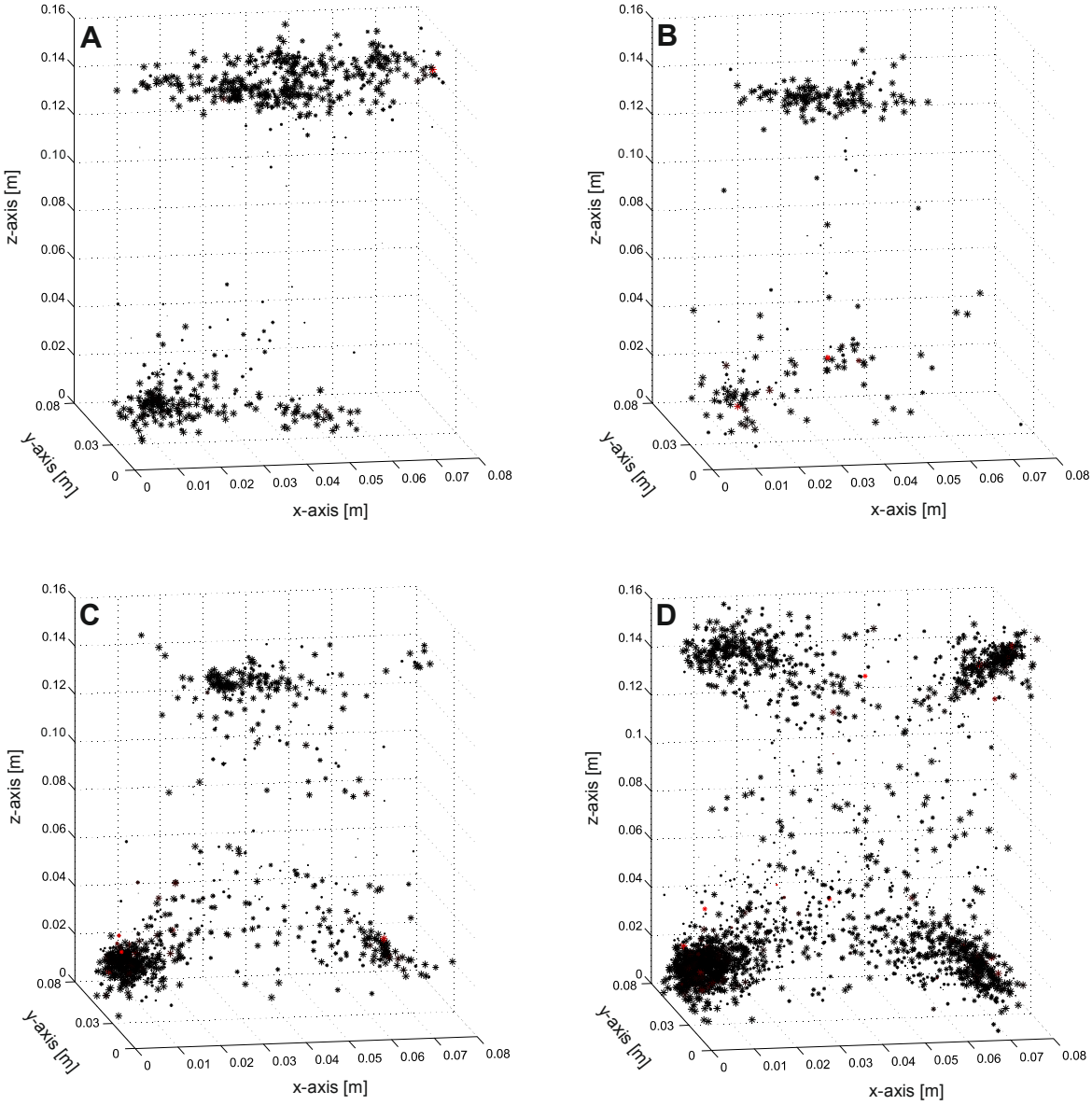

Fig. 4. Localized AE events during crack closure (A), elastic deformation (B), stable crack growth (C) and unstable crack growth (D). Larger markers represent better correlation coefficients, red markers show high event energies.

Especially during the first stage of deformation (A) a concentration of events occurred in the bottom and top of the sample. In this test, no PTFE plates were applied between rock and loading plates and thus the signals can be contributed to friction at the loading plates. In the second stage (B), in total less events were detected as almost no cracks form or propagate during elastic deformation. During stable crack growth more events are located in the middle of the rock cylinder and microcracks are initiated mainly in the form of an hourglass. The hourglass shape of evolving microcracks is characteristic for the fracture pattern observed after unconfined compression due to stress concentrations in the rock. In the stage of unstable crack growth (D) conjugate shear bands start to evolve more clearly but still a lot of signals are located close to the end surfaces.

In the lower left part of the specimen an accumulation of events occurs which already starts in the first stages. Some high energy signals are also located there (red markers). Comparing results from localization to the failure pattern of the tested specimen (Fig. 5, left), we find that no conjugate shear system developed after failure although it was visible in located AE (Fig. 4 D). As shown in Fig. 5, a rock fragment split off at the edge of the sample sub-parallel to the loading direction. The failure occurred on the left side of the rock cylinder where the accumulation of events is located (Fig. 5, right). As the test was stopped immediately after the first major fracture, further macrocracks were restricted which may have formed under continuing loading.

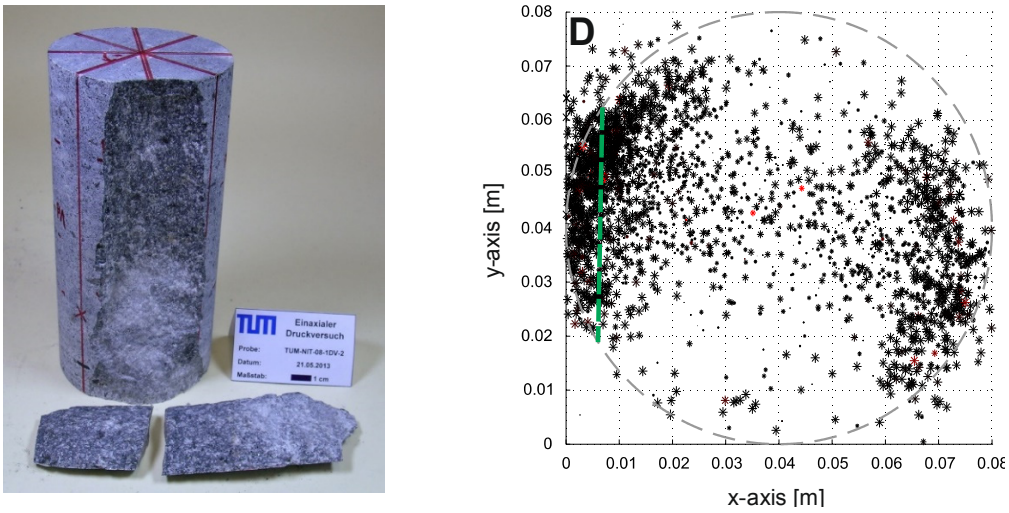

Fig. 5. Left: Final fracture pattern showing one macrocrack aligned parallel to the loading direction. Right: Located AE events during unstable crack growth (D). View in z-direction from the top with an accumulation of events on the left side (green line) where the final fracture occurred.

5. Conclusion

This paper presents results of two unconfined compression tests on homogeneous diorite samples which were combined with AE measurements in order to confirm the applicability and accuracy of the experimental setup. In a preliminary test, the influence of PTFE material as a means for minimizing end effects was investigated. The results showed that although acoustic events were minimized at the end surfaces, the stress-strain curve changed considerably. Without PTFE plates, acoustic events due to friction were clearly visible at the end surfaces.

From the stress-strain curve combined with the number of AE, deformation stages in crack development could be defined. A 3D source localisation of events displays a typical conjugate shear system which developed during unconfined compression testing. In contrast, the final fracture pattern showed a thin rock fragment which split off the rock but did not

reveal the expected conjugate shear planes. Yet, a significant accumulation of events at the edge of the specimen indicated the fracture pattern already before the rock failed.

This study demonstrates that AE analysis represents a practical non-destructive testing technique to show fracture processes inside a homogeneous rock specimen. Further research will focus on stress-induced damage, time-dependent relaxation and their influence on rock strength and deformation properties. For this purpose, AE as well as volumetric strain measurements will be carried out combined with p-wave velocity measurements and petrographic investigations.

References

[1] Hoek, E., Bieniawski, Z.T. (1965): Brittle Rock Fracture Propagation In Rock Under Compression. – Int. J. Fract. Mech., 1 (3): 137-155.

[2] Young, R. P., Martin, C. D. (1993): Potential Role of Acoustic Emission/Microseismicity Investigations in the Site Characterization and Performance Monitoring of Nuclear Waste Repositories. – Int. J. Rock Mech. Min. Sci. & Geomech. Abstr., 30 (7): 797-803.

[3] Bieniawski, Z.T. (1967): Mechanism of brittle fracture of rock. – Int. J. Rock Mech. Min. Sci., 4: 395-406.

[4] Martin, C. D., Read, R. S. & Martino, J. B. (1997): Observation of brittle failure around a circular test tunnel. – Int. J. Rock Mech. Min. Sci., 34 (7): 1065-1073.

[5] Mutschler, T. (2004): Neufassung der Empfehlung Nr. 1 des Arbeitskreises "Versuchstechnik Fels" der Deutschen Gesellschaft für Geotechnik e. V.: Einaxiale Druckversuche an zylindrischen Gesteinsprüfkörpern. – Bautechnik, 81 (10): 825-834.

[6] Grosse C., Ohtsu M. (Eds.) (2010): Acoustic Emission Testing. Basics for Research - Applications in Civil Engineering. – 396 S., Berlin (Springer).

[7] Bancroft, S. (1985): An Algebraic Solution of the GPS Equations. – IEEE Transactions on Aerospace and Electronic Systems, AES-21 (7): 56-59.

[8] Geiger, L. (1910): Herdbestimmung bei Erdbeben aus den Ankunftszeiten. – Kgl. Ges. d. Wiss. Nachrichten. Math.-phys. Klasse (4): 231-349.

[9] Kurz, J. H. (2006): Verifikation von Bruchprozessen bei gleichzeitiger Automatisierung der Schallemissionsanalyse an Stahl- und Stahlfaserbeton. – Diss., Institut für Werkstoffe im Bauwesen, Universität Stuttgart, 197 S.; Stuttgart.

[10] Eberhardt, E., Stead, D. & Stimpson, B. (1999): Quantifying progressive pre-peak brittle fracture damage in rock during uniaxial compression. – Int. J. Rock Mech. Min. Sci., 36: 361-380.

[11] Cai, M., Kaiser, P., Tasaka, Y., Maejima, T., Morioka, H. & Minami, M. (2004): Generalized crack initiation and crack damage stress thresholds of brittle rock masses near underground excavations. – Int. J. Rock Mech. Min. Sci., 41 (5): 833-847.